ACS APPLIED MATERIALS & INTERFACES

Letter

www.acsami.org

Distinguishing Localized Surface Plasmon Resonance and Schottky Junction of Au−Cu_2O Composites by Their Molecular Spacer Dependence

Denghui Jiang,[†,‡] Wei Zhou,[§] Xinhua Zhong,[§] Yuegang Zhang,[∥] and Xinheng Li*[,†,‡]

[†]The Laboratory for Nano-Catalytic Materials and Technologies and [∥]i-Lab, Suzhou Institute of Nano-tech and Nano-bionics, Chinese Academy of Sciences, Suzhou 215123, China

[§]School of Chemistry and Molecular Engineering, East China University of Science and Technology, Shanghai 200237, China

[‡]The State Key Laboratory for Oxo Synthesis and Selective Oxidation, Lanzhou Institute of Chemical Physics, Chinese Academy of Sciences, Lanzhou 730000, China

Supporting Information

ABSTRACT: The surface plasmon resonance (SPR) and Schottky effects are important photocatalytic activity boosters in metallic cocatalyst/photocatalyst systems, but it is difficult to differentiate them. In this report, we design a simple method to distinguish the two effects by utilizing a distance-tunable self-assembled monolayer (SAM) in a gold (Au)−Cu_2O composite in conjunction with UV and visible-light sources, by which we had only the SPR or Schottky effect identified in the visible or UV light, respectively. Cysteine (cys) and mercaptoundecanoic acid (MUA) SAMs as linkers were used respectively for making Au−cys−Cu_2O and Au−MUA−Cu_2O composites. Au−citrate−Cu_2O as a mild linker was also synthesized. Under UV-light irradiation, Au−Cu_2O showed only the Schottky effect, while Au−MUA−Cu_2O and Au−cys−Cu_2O showed neither of the two effects. Under visible-light irradiation, Au−MUA−Cu_2O and Au−cys−Cu_2O showed clearly only the localized SPR (LSPR) effect, while Au−Cu_2O demonstrated the coexistence of the two effects, which was further confirmed by their LSPR enhancement factor.

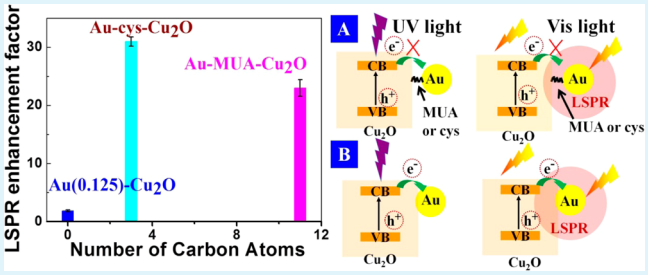

KEYWORDS: *LSPR, Schottky effect, cuprous oxide, self-assembled monolayer, photocatalytic activity*

Photocatalysis and photovoltaics as an alternative green energy have made great progress in the past decade by virtue of the advancement of advanced materials.[1] However, the low charge-separation efficiency of photogenerated electron/hole pairs and poor visible-light absorption still severely constrain their further development especially toward commercial production.[1,2] In view of these scientific problems, strategies such as adopting surface plasmon resonance (SPR) enhancements,[1] building up multijunctions at nanoscale,[1] developing new materials/systems,[2] etc., have been keenly developed. Among those, plasmonic photocatalysts have emerged as a new kind of photocatalysts because of the enhancement effect mediated by propagating SPR or localized SPR (LSPR).[3,5]

A plasmonic photocatalyst is termed as a composite material composed of metal nanoparticles [e.g., gold (Au), silver (Ag)] as cocatalysts and semiconductors as light harvesters because those metals have propagating SPR or LSPR properties.[3] The SPR effect, either propagating SPR or LSPR, can enhance photocatalytic activities. However, its enhancement mechanism is still elusive. In conventional photocatalysts, metal cocatalysts form a Schottky junction at the interface with its counterpart semiconductors.[4] A Schottky junction can speed up charge separation of photogenerated electron/hole pairs via a built-in electric field formed by accumulated space charges, called the Schottky effect. Hence, the cocatalyst has attracted intensive studies in the past decades theoretically and experimentally.[1,5] However, those systems containing SPR metals could also have SPR effects besides the Schottky effect. This would complicate theoretical investigation because exploring the SPR effect often needs sophisticated instruments like ultrafast femtosecond laser systems.[6] Nevertheless, there is no doubt that SPR enhancement is of great importance not only for increasing light absorption but also for improving excitation and separation efficiencies of electron/hole pairs.[7,8] Therefore, we need a simple but straightforward approach to extracting intricate SPR effects for a deeper understanding. To this end, some new materials have been made by inserting insulating inorganic layers between the cocatalysts and photocatalysts.[9−12] They have indeed proven that the SPR effect in such materials greatly boosted photocatalytic activities. However, on the one hand, identifying the SPR effect of diverse materials except for the

Received: April 20, 2014
Accepted: June 30, 2014
Published: June 30, 2014

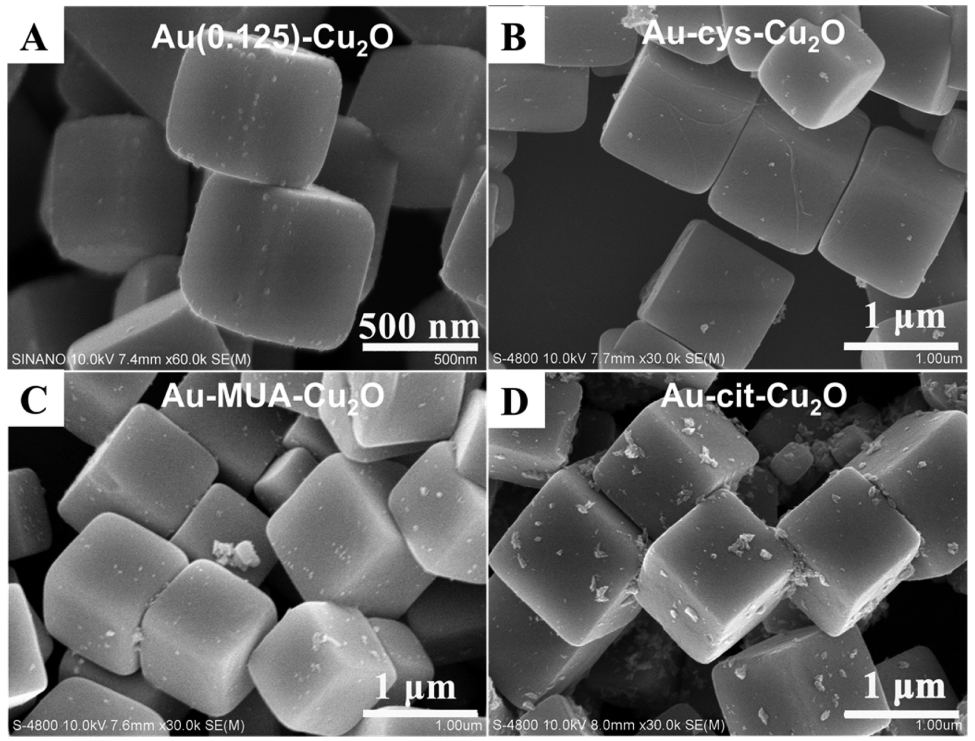

Figure 1. SEM images of the Au(0.125)−Cu_2O (A), Au−cys−Cu_2O (B), Au−MUA−Cu_2O (C), and Au−cit−Cu_2O nanostructures (D).

tailor-made materials is still elusive. On the other hand, in reality, the majority of photocatalytic materials have intimate contacts between cocatalysts and light harvesters. Hence, it is meaningful and indispensible to develop a strategy for identifying the SPR effect in either case.

We chose a Au−Cu_2O cube as our study system. First, as an important p-type semiconductor with a band gap of 2.0−2.2 eV,[7,13] Cu_2O has a visible-light absorption band overlapping with the LSPR peak (ca. 2.38 eV)[8] of Au nanoparticles. Second, Cu_2O has low cost and is environmentally benign, which is suitable for wide potential applications.[4,13−17] Third, it is easy to synthesize and has good chemical stability.[21] A variety of interesting Cu_2O nanostructures such as cube, cuboctahedra, octahedra, nanorod, and hollow structure have been fabricated.[14,15,18−20] Cu_2O cube has the highest chemical stability of all morphologies of cuprous oxide, although its photocatalytic activity is very low.[21] Fourth, in recent years, many efforts have been devoted to making Au−Cu_2O heteronanostructures.[7,8,22−28] For example, Pang et al. have synthesized many complex nanostructures such as core−shell and yolk−shell heterodimers.[26] Zhu et al. have studied the selective growth of Au nanoparticles on specific positions of Cu_2O octahedra.[29] However, reports on the synthesis of Au−Cu_2O cube composites for LSPR enhancement of the photocatalytic activity are rare.

In this paper, we have designed a simple method for identifying the LSPR and Schottky effects. Insulating self-assembled monolayers (SAMs) between Au nanocrystals and cuprous oxide were introduced. Cysteine (cys) and mercaptoundecanoic acid (MUA) SAMs as linkers with different chain lengths were used respectively for making Au−cys−Cu_2O and Au−MUA−Cu_2O cubic composites. Both visible-light (λ > 420 nm) and UV-light (ca. λ = 254 nm) sources were applied to disentangle the two effects, i.e., the LSPR and Schottky effects. Note that a xenon lamp was chosen for Au deposition in order to facilitate photoreduction such that surface oxidation due to galvanic replacement could be effectively hampered.

Four different Au−Cu_2O cubic composites with relatively low Au coverage were synthesized. The Au−Cu_2O composites are classified into three categories, i.e., the intimate-contact case like Au(0.125)−Cu_2O, the no-contact case like Au−cys−Cu_2O and Au−MUA−Cu_2O, and the partial-contact case like Au−citrate (cit)−Cu_2O. The reason for keeping low Au coverage is not to sacrifice adsorption sites of Cu_2O. We tried to keep the surface coverage of Au particles similar. Pristine Cu_2O cubes with an edge length of ca. 585 nm show good monodispersity (Figure S1 in the Supporting Information, SI). X-ray diffraction (XRD) patterns of the obtained Cu_2O reveal sharp Cu_2O peaks, well-matched with the standard spectrum.

Figure 1A shows that Au nanoparticles were relatively evenly distributed on the surfaces of the Cu_2O cubes. The surface density of Au particles is ca. 94 particles/cube, and the size distribution of Au particles is ca. 22 ± 6 nm (Figure S2B in the SI). The high-resolution transmission electron microscopy (HRTEM) image and energy-dispersive spectrometry (EDS) spectrum in Figure S3 in the SI proved the existence of metallic Au. The Au−cys−Cu_2O and Au−MUA−Cu_2O samples are shown in Figure 1B,C. The respective surface densities of the Au particles are ca. 44 and 62 particles/cube, slightly lower than that of Au(0.125)−Cu_2O. Some Au aggregates appeared in the Au−MUA−Cu_2O sample, randomly packing together (Figure S4 in the SI). The presynthesized Au particles had a diameter of ca. 23 nm, analogous to that of Au particles of the Au(0.125)−Cu_2O sample. We ever used the SAM's insulation in measuring Coulomb blockade properties in our previous paper.[30] From the Fourier transform infrared (FTIR) data (Figure S5 in the SI), MUA and cys layers still maintained good stability under UV-light irradiation under our experimental conditions, indicating that our method is feasible. We also made control experiments, i.e., partial-contact case (Au−cit−Cu_2O) in which

Cu_2O somehow contacted with Au particles because of the citrates' loose packing (Figure 1D).[2,31]

Figure S6 in the SI shows the UV−vis absorption spectrum of pristine Cu_2O, where the λ = 478 nm peak is attributed to band absorption and the peak around λ = 550 nm is attributed to scattering.[32] The Au nanoparticle has a strong LSPR peak at λ = 520 nm. Note the LSPR peak of Au in the hybrid samples was not detected largely because of relatively low mass percentage. Because we did not observe big changes of the LSPR peak position and width for the MUA- and cys-passivated Au particles (Figure S7 in the SI), we did not think the surrounding Cu_2O media could have substantial influence on the LSPR peak of Au.

The photocatalytic activities of four different Au−Cu_2O composites were evaluated under UV- and visible-light irradiation for methyl orange (MO) photodegradation. Figure 2A shows that Cu_2O and Au had very few photocatalytic

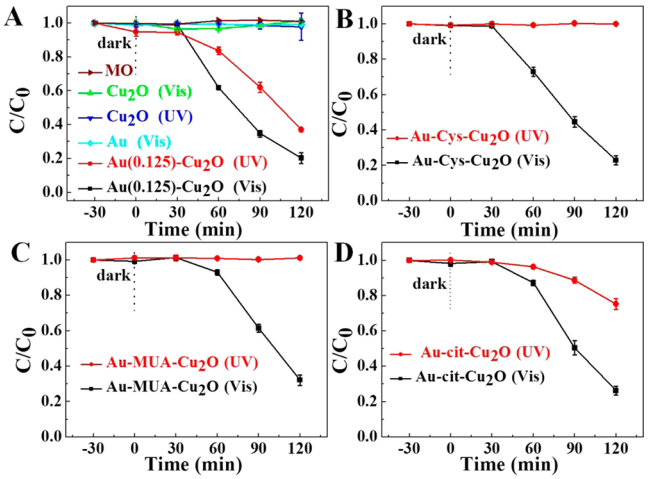

Figure 2. Photocatalytic degradation of MO under UV-light (λ = 254 nm) and visible-light (λ > 420 nm) irradiation by Au(0.125)−Cu_2O (A), Au−cys−Cu_2O (B), Au−MUA−Cu_2O (C), and Au−cit−Cu_2O (D).

activities (less than 1%) under UV- and visible-light irradiation. Note that weak adsorption due to neutral nature of {100} facet and poor hydrophilicity are the main reasons for the reaction to occur slowly in the first 30 min.[14] After that, the reaction showed an intrinsic photocatalytic rate, which was not affected by adsorption. Under UV-light irradiation, the Au(0.125)−Cu_2O sample photodegraded about 63% of MO, while both Au−cys−Cu_2O and Au−MUA−Cu_2O showed almost negligible activity. Under visible-light irradiation, Au−cys−Cu_2O and Au−MUA−Cu_2O photodegraded 80% and 72% of MO. The two no-contact samples showed a better performance under visible light than under UV light. Because they had no Schottky effect, their activity enhancement came solely from the LSPR effect. This proves the feasibility of our method for distinguishing Schottky and LSPR effects. We further tested Au−cit−Cu_2O with partial contact. Under UV-light irradiation, Au−cit−Cu_2O photodegraded ca. 20% of MO. It is much lower than that of Au(0.125)−Cu_2O but much higher than those of Au−cys−Cu_2O and Au−MUA−Cu_2O, suggesting less insulation compared to MUA and cys SAMs. Hence, making use of organic molecular spacers in conjunction with UV- and visible-light sources is proven to be able to distinguish and identify the role of LSPR.

We further applied five different wavelength light sources with narrow band-pass filters for the photocatalytic test (Figure 3A,B). Photocatalytic rates and efficiencies of Au−cys−Cu_2O

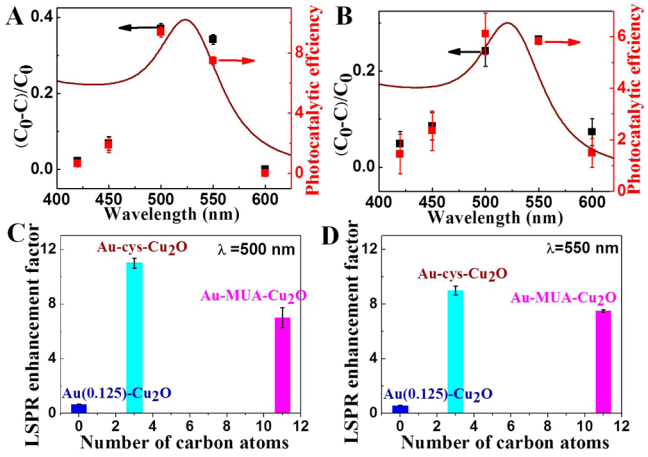

Figure 3. Light wavelength-dependent photocatalytic rates and efficiencies[33] of Au−cys−Cu_2O (A) and Au−MUA−Cu_2O (B). LSPR enhancement factors against the number of carbon atoms at λ = 500 nm (C) and λ = 550 nm (D) light irradiation. Wine-colored curves in A and B are UV−vis absorption spectra of the Au nanoparticles.

and Au−MUA−Cu_2O reached maximal values at λ = 500 and 550 nm, respectively, overlapping with the LSPR band of the Au particles. This is well consistent with a strong LSPR enhancement effect.

We define the LSPR enhancement factor and compared them with each other in Figure 3C,D in order to better describe the LSPR effect in such complicated systems. Herein, we tentatively define the LSPR enhancement factor as the visible-light photocatalytic rate divided by the UV-light photocatalytic rate (Figure S10 in the SI), which were extracted from their corresponding photocatalytic activities based on first-order reaction kinetics. The definition of the LSPR factor is based on the following assumptions: (1) Only the LSPR and Schottky effects are considered in the studied systems. (2) Its contribution to the overall photocatalytic activities is linear. Parts C and D of Figure 3 show that Au−cys−Cu_2O had a larger factor than Au−MUA−Cu_2O. This was further proven by experiments under a full visible-light spectrum irradiation (Figure S8 in the SI). A slightly larger ratio occurred at λ = 500 nm than at λ = 550 nm and may be a sign of a wavelength matching mechanism between the LSPR and absorption peaks of Cu_2O.

The above phenomenon can be well accounted for by the LSPR enhancement mechanism.[1,10] It is well-known that the intensity of the localized electric field exponentially decreases away from Au.[10] MUA has a thickness of ca. 1.6 nm, and cys has a thickness of ca. 0.6 nm, as shown in Figure S9 in the SI. So, cys with a shorter carbon chain length resulted in a stronger localized electric field near the Cu_2O surfaces than MUA, resulting in higher photocatalytic activity.

In order to further confirm the relationship between the LSPR and Schottky effects, Au−Cu_2O composites with different Au loading amounts were compared. Parts A and B of Figure 4 show an apparent increase of the number of Au nanoparticles on the surfaces of the Cu_2O cubes. Under UV-light irradiation, the Au(0.25)−Cu_2O photocatalytic rate was

dx.doi.org/10.1021/am5023978 | ACS Appl. Mater. Interfaces 2014, 6, 10958−10962

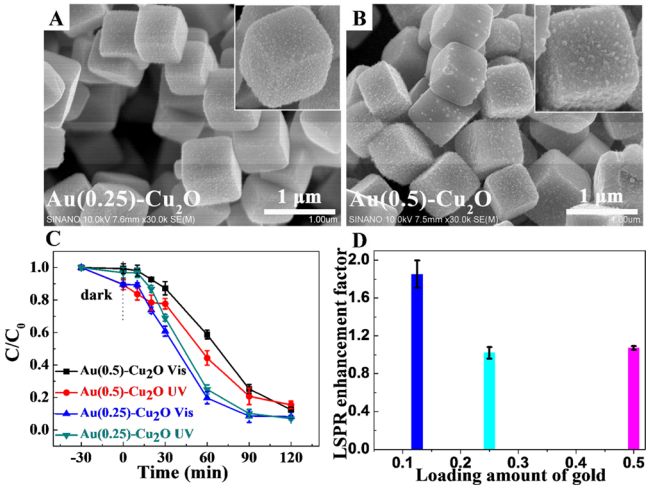

Figure 4. SEM images of the Au(0.25)−Cu_2O (A) and Au(0.5)−Cu_2O (B) composites. Photocatalytic activities of MO of Au(0.25)−Cu_2O and Au(0.5)−Cu_2O under UV- and visible-light irradiation (C). LSPR enhancement factor against the Au loading amount (D).

higher than that of Au(0.125)−Cu_2O (Figure 4C), consistent with Schottky-effect-dominated trends. However, we found that the photocatalytic rate declined after the Au loading amount reached beyond 0.5 (Figure S10 in the SI). We attributed the decline to adsorption blockage, i.e., excessive Au occupied a large amount of adsorption sites of Cu_2O.

To exclude a possible blocking effect (negative effect), we did a series of control experiments, summarized in Figure S10 in the SI. The Au(5.0)−Cu_2O photocatalytic activity significantly declined, explicitly indicating that a blocking effect occurred. Au(0.5)−Cu_2O and Au(0.75)−Cu_2O had similar rates but slightly declined compared to Au(0.25)−Cu_2O, indicating that they were in a threshold window. So, it is reasonable to use Au(0.125)−Cu_2O and Au(0.25)−Cu_2O for comparison. The LSPR enhancement factor against the Au loading amount is plotted in Figure 4D. According to the diagram, the LSPR factor decreased with an increase in the Au amount without blocking adsorption sites of the reactants. We have further studied the photocatalytic stability of the Au−Cu_2O photocatalyst (Figure S11 in the SI). After five cycles of the photodegradation test, no significant loss of the photocatalytic activity was observed. Besides cubic morphology, Cu^{I} still remained and no Cu^{II} formed.

On the basis of the above results, we proposed the charge-transfer mechanism shown in Figure S12 in the SI. As for the molecular spacers, sulfur was attached to Au, while a carboxylic anion was attached to cuprous oxide via covalent bonding.[31] The alkane chains with different lengths between them are insulating. So, cys and MUA behaved as electron-transfer blockers such that hot electron transfer or tunneling through the cys or MUA SAM got pretty difficult. Subsequently, the LSPR effect became predominant under visible light. Additionally, it is known that the LSPR effect is strongly dependent on the spacer distance with an exponential relationship. So, MUA had a smaller LSPR enhancement factor than cys. With an increase of the Au coverage density of Au−Cu_2O, more Schottky junctions formed and more excited electrons injected into the Fermi level of Au nanoparticles.[1] The LSPR share decrease indicated that the Schottky effect may compete with LSPR. Moreover, different LSPR enhancement factors for Au−cys−Cu_2O and Au−MUA−Cu_2O with similar Au surface densities suggest that LSPR might also speed up charge separation besides enhancing light absorption. Additionally, cys and MUA have light absorption in the deep-UV region. However, from our experimental results, we did not observe a noticeable effect on their corresponding photocatalytic performance. At the same time, we also did not observe the effect of the d-band transition of Au nanoparticles.[34]

We have designed a simple method for differentiating photocatalysts' LSPR and Schottky effects. In this method, we introduced an insulating SAM between the Au nanocrystal and cuprous oxide in conjunction with UV- and visible-light sources. cys and MUA SAMs as linkers were used respectively for making Au−cys−Cu_2O and Au−MUA−Cu_2O with relatively low Au coverage. Cu_2O and Au have an overlap in their absorption spectra. Under UV-light irradiation, Au−Cu_2O showed only the Schottky effect, while Au−MUA−Cu_2O and Au−cys−Cu_2O showed no considerable effects. Under visible-light irradiation, Au−MUA−Cu_2O and Au−cys−Cu_2O showed clearly only the LSPR effect, while Au−Cu_2O demonstrated the coexistence of the two effects, which was further confirmed by their LSPR enhancement factor. The approximated LSPR enhancement factor against the number of carbon atoms further reveals that cys presented a more maximal LSPR factor enhancement than MUA, consistent with the LSPR mechanism. We also made Au−cit−Cu_2O with partial contact the control experiment. Regarding intimate contact, with increasing loading amount of Au, we found that the role of LSPR enhancement remained but its share tended to decrease, suggesting that the LSPR effect may compete with the Schottky effect. This approach can be extended to other similar systems for a deeper understanding of the effect of LSPR and its interaction with excitons. This work provides a simple method for the future design and development of efficient composite plasmonic photocatalysts toward higher performance.

■ ASSOCIATED CONTENT

Supporting Information

Further details of experimental methods, particle-size distribution of Au nanoparticles, SEM image, XRD pattern and UV−vis absorption spectrum of the different samples, TEM images and EDX of Au−MUA−Cu_2O and Au−Cu_2O, LSPR enhancement of different Au−Cu_2O composites under a full visible-light spectrum irradiation, FTIR spectra of Au−cys (or MUA)−Cu_2O before and after UV irradiation, molecular structures of MUA, cys, and citric acid, and data fitting for photodegradation. This material is available free of charge via the Internet at http://pubs.acs.org.

■ AUTHOR INFORMATION

Corresponding Author

*E-mail: xinhengli@licp.cas.cn or xhli2012@sinano.ac.cn.

Notes

The authors declare no competing financial interest.

■ ACKNOWLEDGMENTS

X.L. acknowledges financial support from the OSSO State Key Laboratory Project O80117MKJZ by the Ministry of Science and Technology of China.

■ REFERENCES

(1) Zhang, X.; Chen, Y. L.; Liu, R.-S.; Tsai, D. P. Plasmonic Photocatalysis. *Rep. Prog. Phys.* **2013**, *76*, 046401.

(2) Ji, X.; Song, X.; Li, J.; Bai, Y.; Yang, W.; Peng, X. Size Control of Gold Nanocrystals in Citrate Reduction: The Third Role of Citrate. *J. Am. Chem. Soc.* **2007**, *129*, 13939−13948.
(3) Xiao, M.; Jiang, R.; Wang, F.; Fang, C.; Wang, J.; Yu, J. C. Plasmon-Enhanced Chemical Reactions. *J. Mater. Chem. A* **2013**, *1*, 5790−5805.
(4) Zhang, J.; Liu, J.; Peng, Q.; Wang, X.; Li, Y. Nearly Monodisperse Cu_2O and CuO Nanospheres: Preparation and Applications for Sensitive Gas Sensors. *Chem. Mater.* **2006**, *18*, 867−871.
(5) Gou, L.; Murphy, C. J. Controlling the Size of Cu_2O Nanocubes from 200 to 25 nm. *J. Mater. Chem.* **2004**, *14*, 735−738.
(6) Plech, A.; Leiderer, P.; Boneberg, J. Femtosecond Laser Near Field Ablation. *Laser Photonics Rev.* **2009**, *3*, 435−451.
(7) Mahmoud, M. A.; Qian, W.; El-Sayed, M. A. Following Charge Separation on the Nanoscale in Cu_2O−Au Nanoframe Hollow Nanoparticles. *Nano Lett.* **2011**, *11*, 3285−3289.
(8) Cushing, S. K.; Li, J.; Meng, F.; Senty, T. R.; Suri, S.; Zhi, M.; Li, M.; Bristow, A. D.; Wu, N. Photocatalytic Activity Enhanced by Plasmonic Resonant Energy Transfer from Metal to Semiconductor. *J. Am. Chem. Soc.* **2012**, *134*, 15033−15041.
(9) Awazu, K.; Fujimaki, M.; Rockstuhl, C.; Tominaga, J.; Murakami, H.; Ohki, Y.; Yoshida, N.; Watanabe, T. A Plasmonic Photocatalyst Consisting of Silver Nanoparticles Embedded in Titanium Dioxide. *J. Am. Chem. Soc.* **2008**, *130*, 1676−1680.
(10) Kumar, M. K.; Krishnamoorthy, S.; Tan, L. K.; Chiam, S. Y.; Tripathy, S.; Gao, H. Field Effects in Plasmonic Photocatalyst by Precise SiO_2 Thickness Control Using Atomic Layer Deposition. *ACS Catal.* **2011**, *1*, 300−308.
(11) Torimoto, T.; Horibe, H.; Kameyama, T.; Okazaki, K.-i.; Ikeda, S.; Matsumura, M.; Ishikawa, A.; Ishihara, H. Plasmon-Enhanced Photocatalytic Activity of Cadmium Sulfide Nanoparticle Immobilized on Silica-Coated Gold Particles. *J. Phys. Chem. Lett.* **2011**, *2*, 2057−2062.
(12) Chen, J.-J.; Wu, J. C. S.; Wu, P. C.; Tsai, D. P. Improved Photocatalytic Activity of Shell-Isolated Plasmonic Photocatalyst Au@SiO_2/TiO_2 by Promoted LSPR. *J. Phys. Chem. C* **2012**, *116*, 26535−26542.
(13) Fernando, C. A. N.; de Silva, P. H. C.; Wethasinha, S. K.; Dharmadasa, I. M.; Delsol, T.; Simmonds, M. C. Investigation of n-Type Cu_2O Layers Prepared by a Low Cost Chemical Method for Use in Photovoltaic Thin Film Solar Cells. *Renewable Energy* **2002**, *26*, 521−529.
(14) Huang, W.-C.; Lyu, L.-M.; Yang, Y.-C.; Huang, M. H. Synthesis of Cu_2O Nanocrystals from Cubic to Rhombic Dodecahedral Structures and Their Comparative Photocatalytic Activity. *J. Am. Chem. Soc.* **2012**, *134*, 1261−1267.
(15) Gomes Silva, C.; Juárez, R.; Marino, T.; Molinari, R.; García, H. Influence of Excitation Wavelength (UV or Visible Light) on the Photocatalytic Activity of Titania Containing Gold Nanoparticles for the Generation of Hydrogen or Oxygen from Water. *J. Am. Chem. Soc.* **2011**, *133*, 595−602.
(16) Hara, M.; Kondo, T.; Komoda, M.; Ikeda, S.; Kondo, J.; Domen, K.; Hara, M.; Shinohara, K.; Tanaka, A. Cu_2O as a Photocatalyst for Overall Water Splitting under Visible Light Irradiation. *Chem. Commun.* **1998**, 357−358.
(17) Zhang, D.-F.; Zhang, H.; Guo, L.; Zheng, K.; Han, X.-D.; Zhang, Z. Delicate Control of Crystallographic Facet-Oriented Cu_2O Nanocrystals and the Correlated Adsorption Ability. *J. Mater. Chem.* **2009**, *19*, 5220−5225.
(18) Kuo, C.-H.; Huang, M. H. Morphologically Controlled Synthesis of Cu_2O Nanocrystals and Their Properties. *Nano Today* **2010**, *5*, 106−116.
(19) Corma, A.; Garcia, H. Supported Gold Nanoparticles as Catalysts for Organic Reactions. *Chem. Soc. Rev.* **2008**, *37*, 2096−2126.
(20) Tan, Y.; Xue, X.; Peng, Q.; Zhao, H.; Wang, T.; Li, Y. Controllable Fabrication and Electrical Performance of Single Crystalline Cu_2O Nanowires with High Aspect Ratios. *Nano Lett.* **2007**, *7*, 3723−3728.
(21) Hua, Q.; Shang, D.; Zhang, W.; Chen, K.; Chang, S.; Ma, Y.; Jiang, Z.; Yang, J.; Huang, W. Morphological Evolution of Cu_2O Nanocrystals in an Acid Solution: Stability of Different Crystal Planes. *Langmuir* **2011**, *27*, 665−671.
(22) Kuo, C.-H.; Yang, Y.-C.; Guo, S.; Huang, M. H. Facet-Dependent and Au Nanocrystal-Enhanced Electrical and Photocatalytic Properties of Au−Cu_2O Core−Shell Heterostructures. *J. Am. Chem. Soc.* **2011**, *133*, 1052−1057.
(23) Wang, W.-C.; Lyu, L.-M.; Huang, M. H. Investigation of the Effects of Polyhedral Gold Nanocrystal Morphology and Facets on the Formation of Au−Cu_2O Core−Shell Heterostructures. *Chem. Mater.* **2011**, *23*, 2677−2684.
(24) Wang, Z.; Zhao, S.; Zhu, S.; Sun, Y.; Fang, M. Photocatalytic Synthesis of M/Cu_2O (M = Ag, Au) Heterogeneous Nanocrystals and Their Photocatalytic Properties. *CrystEngComm* **2011**, *13*, 2262−2267.
(25) Kong, L.; Chen, W.; Ma, D.; Yang, Y.; Liu, S.; Huang, S. Size Control of Au@Cu_2O Octahedra for Excellent Photocatalytic Performance. *J. Mater. Chem.* **2012**, *22*, 719−724.
(26) Pang, M.; Wang, Q.; Zeng, H. C. Self-Generated Etchant for Synthetic Sculpturing of Cu_2O−Au, Cu_2O@Au, Au/Cu_2O, and 3D-Au Nanostructures. *Chem.—Eur. J.* **2012**, *18*, 14605−14609.
(27) Pan, Y.; Deng, S.; Polavarapu, L.; Gao, N.; Yuan, P.; Sow, C. H.; Xu, Q.-H. Plasmon-Enhanced Photocatalytic Properties of Cu_2O Nanowire−Au Nanoparticle Assemblies. *Langmuir* **2012**, *28*, 12304−12310.
(28) Zhang, L.; Blom, D. A.; Wang, H. Au−Cu_2O Core−Shell Nanoparticles: A Hybrid Metal−Semiconductor Heteronanostructure with Geometrically Tunable Optical Properties. *Chem. Mater.* **2011**, *23*, 4587−4598.
(29) Zhu, H.; Du, M.; Yu, D.; Wang, Y.; Wang, L.; Zou, M.; Zhang, M.; Fu, Y. A New Strategy for the Surface-Free-Energy-Distribution Induced Selective Growth and Controlled Formation of Cu_2O−Au Hierarchical Heterostructures with a Series of Morphological Evolutions. *J. Mater. Chem. A* **2013**, *1*, 919−929.
(30) Li, X.; Yasutake, Y.; Kono, K.; Kanehara, M.; Teranishi, T.; Majima, Y. Au Nanoparticles Chemisorbed by Dithiol Molecules Inserted in Alkanethiol Self-Assembled Monolayers Characterized by Scanning Tunneling Microscopy. *Jpn. J. Appl. Phys.* **2009**, *48*, 04C180.
(31) Saha, K.; Agasti, S. S.; Kim, C.; Li, X.; Rotello, V. M. Gold Nanoparticles in Chemical and Biological Sensing. *Chem. Rev.* **2012**, *112*, 2739−2779.
(32) Liang, X.; Gao, L.; Yang, S.; Sun, J. Facile Synthesis and Shape Evolution of Single-Crystal Cuprous Oxide. *Adv. Mater.* **2009**, *21*, 2068−2071.
(33) Li, J.; Cushing, S. K.; Bright, J.; Meng, F.; Senty, T. R.; Zheng, P.; Bristow, A. D.; Wu, N. Ag@Cu_2O Core−Shell Nanoparticles as Visible-Light Plasmonic Photocatalysts. *ACS Catal.* **2013**, *3*, 47−51.
(34) Ahmadi, T. S.; Logunov, S. L.; El-Sayed, M. A. Picosecond Dynamics of Colloidal Gold Nanoparticles. *J. Phys. Chem.* **1996**, *100*, 8053−8056.